In-Situ Formation of Silver Nanoparticles with Tunable Spatial Distribution at the Poly(*N*-isopropylacrylamide) Corona of Unimolecular Micelles

Hangxun Xu, Jian Xu, Zhiyuan Zhu, Hewen Liu, and Shiyong Liu*

Department of Polymer Science and Engineering, the Hefei National Laboratory for Physical Sciences at Microscale, Hefei, 230026 Anhui Province, China

Received July 14, 2006; Revised Manuscript Received August 29, 2006

ABSTRACT: Highly stable hybrid unimolecular micelles with thermosensitive poly(*N*-isopropylacrylamide) (PNIPAM) shells incorporated with Ag nanoparticles were prepared in situ via a facile approach. Heating the hybrid unimolecular micellar solutions leads to the shrinkage of the PNIPAM shell and allows for tuning the relative spatial distances between neighboring Ag nanoparticles. Because of the anchoring and stabilization of PNIPAM brush to the Ag nanoparticles, the tuning of spatial distribution of nanoparticles within the unimolecular micelles is completely reversible with heating/cooling cycles. The facile preparation procedures and their efficiency of response to the surrounding media render these novel hybrid unimolecular micelles potential candidates for applications in sensors, catalysis, and optic/electronic devices.

The versatility of physical and chemical properties of metal and semiconductor nanoparticles render them as promising materials in the fields ranging from optoelectronics[1] and sensors[2] to catalysis[3] and medicine.[4] So far, great research interests have involved in fabricating nanoparticle assemblies as they represent a popular route toward the preparation of advanced functional materials as well as a central concept in nanoscience and nanotechnology.[5] To this end, polymer−nanoparticle composites are promising candidates with the purpose to exploit or enhance the unique properties of nanoparticles while the polymer matrix can control host−guest interactions to ensure the well-defined spatial distribution of nanoparticles. The immobilization of metal nanoparticles in a polymeric matrix such as block copolymer micelles,[6] dendrimers,[7] latex particles,[8] and microgels[9] provides a convenient approach for the fabrication of morphologically controlled and highly ordered arrays of metal nanoparticles. However, in most cases, the polymer matrix only serves as a suitable scaffold for immobilizing the nanoparticles and preventing them from aggregation. In some specific applications, it would be highly desirable to modulate the spatial distribution between nanoparticles and the permeability of the polymer carrier to external chemical or biochemical species.

Thermosensitive microgels have been used as templates for the preparation of gold or silver nanoparticles with tunable spatial distribution and adjustable catalytic activities.[10] As compared to microgels, block copolymer micelles offer more versatile templating and adjustable loading capacities via the variation of relative block lengths as well as the composition.[11] However, block copolymer micelles exist in thermodynamic equilibrium with unimers in the solution, and they tend to be disintegrated upon dilution and change of external conditions. When hydrophilic polymer chains are tethered to a hydrophobic multifunctional core, such as dendritic macromolecules and multiarm star copolymers, they can be considered as unimolecular micelles due to their structural resemblance to the amphiphilic block copolymer micelles.[12] They generally possess well-defined chemical structures with predetermined core size, controllable length, and density of grafted chains; thus, they could also serve as highly stable templates for the preparation of hybrid metal nanoparticles.

Herein we present the first report of employing thermosensitive unimolecular micelles as templates for the in-situ preparation of silver nanoparticles with controllable spatial distribution. The principle is schematically shown in Figure 1. Silver nanoparticles were in situ generated at the thermoresponsive shell of unimolecular micelles. The core of the micellar carrier consists of fractionated Boltorn H40, a fourth generation of hyperbranched polyester, and the shell consists of densely grafted poly(*N*-isopropylacrylamide) (PNIPAM) chains. Controlling the spatial distribution of silver nanoparticles inside the unimolecular micelles is achieved by taking advantage of the phase transition of PNIPAM shell at its lower critical solution temperature (LCST) of ∼32 °C.[13] At low temperatures, the PNIPAM shell is water-swollen and the embedded nanoparticles are fully accessible to external chemical or biochemical species, while at temperatures above the LCST, the polymer shell collapses. The average spatial distance between silver nanoparticles decreases, and the permeability of the polymer shell reduces considerably. Our previous studies of the H40-PNIPAM unimolecular micelles have demonstrated that the thermal phase transition of PNIPAM shell is completely reversible.[14]

Experimental Section

Materials. Hyperbranched polyester Boltorn H40 was obtained from Perstorp Polyols AB. It was further fractionated with a typical 20% yield using a procedure reported by Tsukruk et al.[15] Boltorn H40 as an ideal dendrimer would theoretically have 64 primary hydroxyl groups and a molar mass of 7316 g mol^{-1}; its ideal chemical structure is shown in Figure 2a. SEC analysis of fractionated Boltorn H40 indicates a $M_n \sim 6500$ g mol^{-1} and polydispersity of 1.40.[14] We denote the fractionated hyperbranched polyester as H40 here. According to Tsukruk et al.,[15b] the degree of branching of H40 was 0.4 and the average number of monomeric units (the degree of polymerization) was ca. 60. *N*-Isopropylacrylamide (97%, Tokyo Kasei Kagyo Co.) was purified by recrystallization in a benzene/*n*-hexane mixture. Silver nitrate ($AgNO_3$, Aldrich) and sodium borohydride ($NaBH_4$, Aldrich) were used as received.

Synthesis of H40-PNIPAM.[14] The general procedure for synthesizing H40-PNIPAM was as follows. A glass ampule was

* To whom correspondence should be addressed. E-mail: sliu@ustc.edu.cn.

10.1021/ma061584d CCC: $33.50
Published on Web 10/25/2006

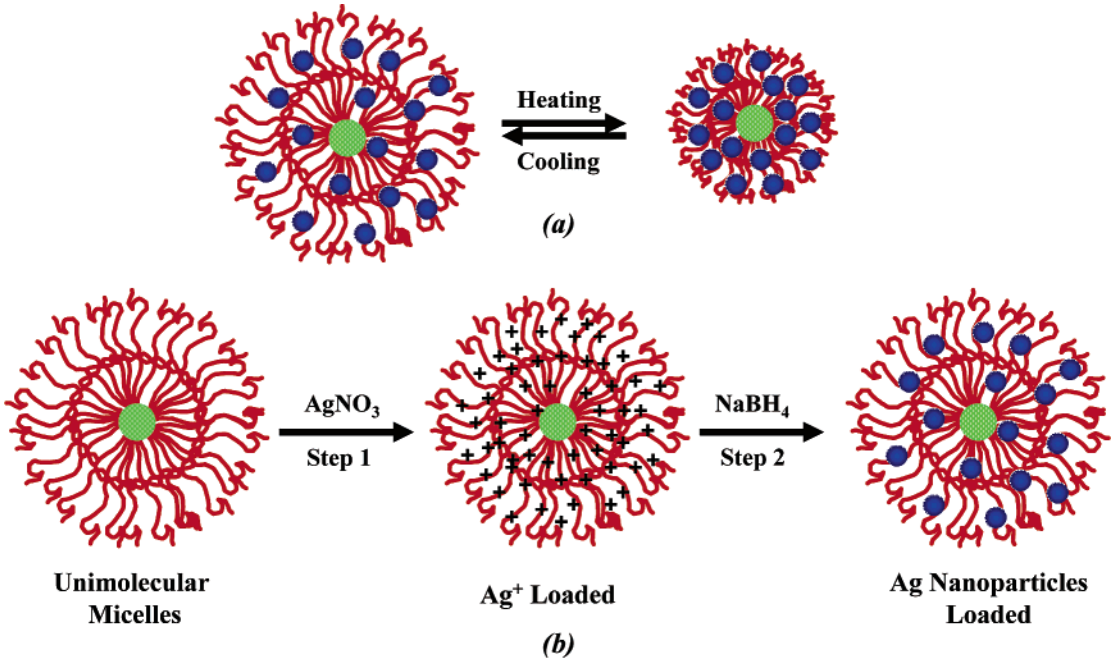

Figure 1. (a) Hybrid unimolecular micelles exhibiting thermotunable spatial distances between Ag nanoparticles. (b) A schematic illustration of the two-step in-situ preparation of hybrid unimolecular micelles incorporated with Ag nanoparticles.

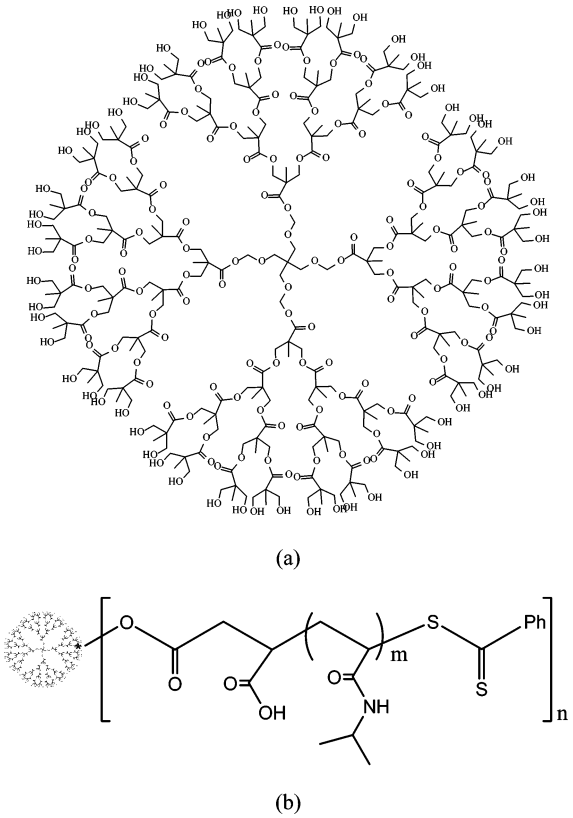

Figure 2. (a) Idealized molecular structure of H40 and (b) the chemical structure of H40-PNIPAM.

charged with H40 macroRAFT agent, AIBN, and NIPAM in THF; it was then degassed by three freeze−thaw cycles and sealed under vacuum. The polymerization was carried out at 80 °C for 12 h. The mixture was precipitated into anhydrous diethyl ether twice. The product was collected by filtration and then dried in a vacuum oven at room temperature. The chemical structure of H40-PNIPAM is shown in Figure 2b.

Cleavage of Grafted PNIPAM Chains.[16] 0.5 g of H40-PNIPAM was dissolved in 100 mL of anhydrous THF; excess lithium chloride and potassium borohydride were slowly added to the solution. The reaction was refluxed with vigorous stirring under nitrogen until the evolution of gas ceased. After the solvent was removed under reduced pressure, the residue was dissolved in methylene chloride and an equal volume of water added. This mixture was extracted three times with methylene chloride, and the organic layers were collected and combined. After concentrating the solution, it was then precipitated in diethyl ether for three times. The cleaved thiol-end functionalized PNIPAM[17a] was dried in a vacuum oven overnight at room temperature. The above reduction procedure degraded the hyperbranched polyester core and recovers the grafted PNIPAM for further SEC characterization.

Characterization of H40-PNIPAM. Size exclusion chromatography (SEC) analysis in DMF of H40-PNIPAM used in this work gives a symmetric elution peak with a number-average molecular weight, M_n, of 9.2×10^5 g/mol and a polydispersity of 1.21. Because of the fact that SEC analysis uses linear polystyrene as standards and that H40-PNIPAM take a dendritic conformation, static LLS was used to determine the absolute molecular weight of H40-PNIPAM. The apparent weight-average molecular weight ($M_{w,app}$) determined by LLS in water was 1.56×10^6 g mol^{-1}. To determine the actual molecular weight of the PNIPAM arm and grafting density, PNIPAM was cleaved from H40-PNIPAM through reduction and purification; SEC analysis of the recovered PNIPAM revealed a M_n of 2.49×10^4 g mol^{-1} and a polydispersity of 1.24, and the degree of polymerization (DP) of PNIPAM arm was then calculated to be ~220. Considering that the $M_{w,app}$ of H40-PNIPAM is 1.56×10^6 g mol^{-1}, the number of PNIPAM arms grafted onto the H40 core is calculated to be ~50.

Fabrication of Hybrid Unimolecular Micelles. The in-situ formation of silver nanoparticles at the corona of unimolecular micelles was carried out by the addition of $AgNO_3$ solution into H40-PNIPAM aqueous solution and subsequent reduction with $NaBH_4$. For a typical example, 5 mg of H40-PNIPAM was dissolved in 20 mL of deionized water; an aqueous solution of 0.024 M $AgNO_3$ (0.5 mL: low dosage; 1.2 mL: high dosage) was then added. After gently stirring for 20 min in the dark at 20 °C, the solution was subjected to dialysis against deionized water for 30 min. An aliquot of aqueous solution of $NaBH_4$ (18 mg in 0.5 mL of water) was then quickly added, and stirring was continued for 4 h. The silver hybrid composite nanoparticles solution was further purified via dialysis against water for 24 h at room temperature.

Instrumentation and Characterization. Molecular weight distributions were determined by SEC using a series of three linear

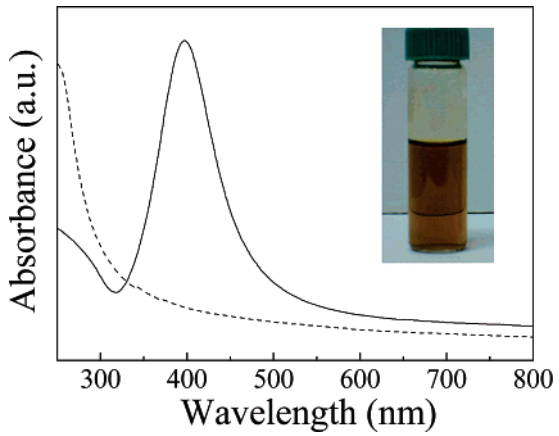

Figure 3. UV−vis spectra of H40-PNIPAM/$AgNO_3$ mixed solutions at high dosage before (dashed line) and after (solid line) reduction with $NaBH_4$. The concentration of H40-PNIPAM was 1×10^{-5} g/mL.

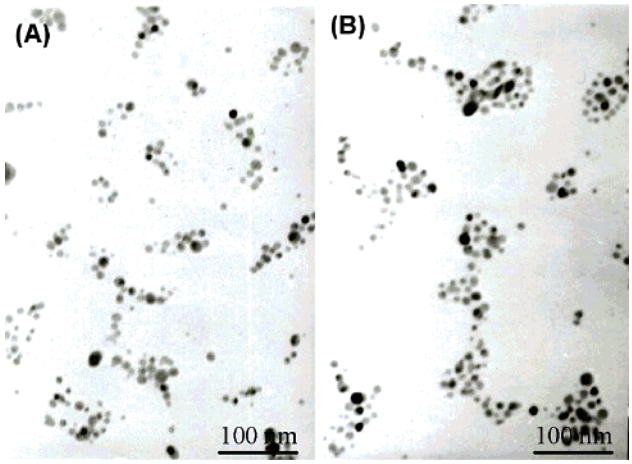

Figure 4. TEM images of the silver composite nanoparticles prepared with different dosages of $AgNO_3$ (A: low dosage; B: high dosage).

Styragel columns HT3, HT4, and HT5 and an oven temperature of 60 °C. A Waters 1515 pump and a Waters 2414 differential refractive index detector (set at 30 °C) were used. The eluent was DMF + 1 g/L BrLi at a flow rate of 1.0 mL/min. Polystyrene standards are used for calibration. Laser light scattering (LLS) was conducted on a commercial spectrometer (ALV/DLS/SLS-5022F) equipped with a multitau digital time correlator (ALV5000) and a cylindrical 22 mW UNIPHASE He−Ne laser ($\lambda_0 = 632$ nm) as the light source was used. Transmission electron microscopy (TEM) analyses were conducted on a Hitachi 800 transmission electron microscope at an acceleration of voltage of 200 kV. The sample for TEM observations was prepared by placing 10 μL of hybrid unimolecular micelles solutions on copper grids coated with thin films of Formvar and carbon successively. UV−vis absorption spectra were recorded with a computer-controlled UNICO UV/vis 2802 PCS spectrophotometer.

Results and Discussion

Dendritic H40-PNIPAM was synthesized via reversible addition−fragmentation chain transfer (RAFT) polymerization of *N*-isopropylacrylamide (NIPAM) using macroRAFT agent based H40. From a structural point of view, dendritic H40-PNIPAM in aqueous solution will exist as unimolecular micelles with H40 as the core and PNIPAM as the shell.

For the in-situ generation of silver nanoparticles at the PNIPAM shell of unimolecular micelles (Figure 1b), aqueous solution of H40-PNIPAM was first treated with $AgNO_3$ solution, and the reduction into Ag nanoparticles was achieved upon addition of excess aqueous solution of $NaBH_4$. The solution immediately turned brownish-yellow. Figure 3 shows the UV−vis absorption spectra before and after reduction.

After the addition of $NaBH_4$, the absorption spectrum displays a significant surface plasmon band at ~398 nm. This band is characteristic of metallic silver colloids.[18] Kumacheva et al.[9a] and Ballauff et al.[8b,19] obtained similar results for silver nanoparticles prepared in the interior of microgels. The sharp peak at ~398 nm thus indicates that silver nanoparticles with a relatively narrow size distribution have been formed inside the polymer shell of unimolecular micelles.

The diameters of the Ag nanoparticles prepared are 6 ± 2 nm as determined from the TEM images shown in Figure 4. Moreover, we can clearly observe a cluster-like distribution of Ag nanoparticles, and isolated nanoparticles are barely observed. From the TEM images, we cannot discern the hydrophobic H40 core. The size of the H40 core is ~3 nm,[15] which is smaller than the mean diameter of the Ag nanoparticles (~6 nm). This indicates that almost all nanoparticles are immobilized within the PNIPAM shell of unimolecular micelles, which is reasonable considering that excess $AgNO_3$ is removed and the PNIPAM chains form quite dense polymer brush. This observation also suggests the preferential localization of Ag^+ ions within the shell due to the complexation of Ag^+ ions by the nitrogen atoms of PNIPAM chains.[8a,b]

From TEM images in Figure 4, we can tell that the number density of silver nanoparticles embedded inside each unimolecular micelles depends on the dosage of $AgNO_3$. For different dosage of $AgNO_3$, the size of silver nanoparticles keeps almost constant at ~6 nm. At high dosage, the average number density of silver nanoparticles inside each unimolecular micelle considerably increases as compared to that at low dosage. The size of clusters of silver nanoparticles is in the range 40−90 nm, which is comparable to the size of unimolecular micelles in the dry state.

The prepared hybrid unimolecular micelles incorporated with Ag nanoparticles are highly stable at room temperature, and we do not observe any precipitation over a period of more than 2 months. In the control experiments without unimolecular micelles as templates, silver nanoparticles were not prepared, and we observe black sediments immediately after addition of $NaBH_4$. The stability of silver composite nanoparticles over long storage again confirms that the nanoparticles were immobilized inside the PNIPAM shell of unimolecular micelles. The grafting density at the surface of H40 core is calculated to be ~0.57 nm^2 per PNIPAM chain. It is reasonable to expect that the densely packed PNIPAM brush and the complexation between Ag nanoparticles and PNIPAM chains both contribute to the stabilization of Ag nanoparticles within the polymer shell.

The PNIPAM shell of unimolecular micelles is thermoresponsive and will collapse at temperatures higher than the LCST. Figure 5 shows the temperature dependence of the average hydrodynamic radius, $\langle R_h \rangle$, of H40-PNIPAM unimolecular micelles and hybrid unimolecular micelles. In both cases, the shrinking of the PNIPAM shell takes place at ~32 °C, which can be ascribed to the thermal phase transition of PNIPAM brush. At low temperatures, the size of the hybrid unimolecular micelles is ~5 nm smaller than that of the original unimolecular micelles. This suggests the quite strong complexation of Ag nanoparticles to the PNIPAM shell and the fact that that nanoparticles act as physical cross-linkers of the shell.[9c] The shrinkage of the hybrid unimolecular micelles is more gradual and less prominent than that of the original unimolecular micelles, reflecting that the incorporation of Ag nanoparticles partially restricts the collapsing at temperatures above the LCST

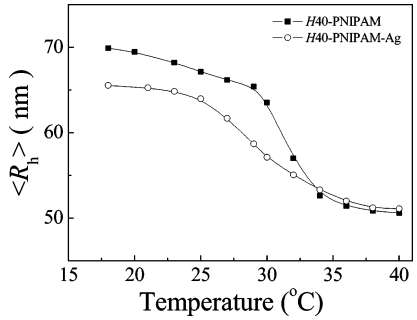

Figure 5. Variation of the average hydrodynamic radius, $\langle R_h \rangle$, of the original unimolecular micelles and hybrid unimolecular micelles (high dosage of $AgNO_3$) as a function of temperature. The concentration of H40-PNIPAM was 1×10^{-5} g/mL.

of PNIPAM.[9c] During the LLS studies, the concentration of H40-PNIPAM is quite low (1×10^{-5} g/mL). Upon heating, we observe the collapse of the PNIPAM brushes on the isolated unimolecular micelles and the closer proximity of embedded Ag nanoparticles. No apparent intermicellar aggregation is observed, and this is in agreement with the phase transition behavior of the original H40-PNIPAM unimolecular micelles.[14] However, at a much higher concentration of 1×10^{-3} g/mL, heating the hybrid unimolecular micelle solution to above the phase transition temperature leads to macroscopic phase separation due to the aggregation of unimolecular micelles. Upon cooling back to 20 °C, the turbid solution becomes clear again.

At lower temperatures, silver nanoparticles immobilized in the unimolecular micelles are well-separated from each other, and the relative distances between nanoparticles will decrease considerably as the PNIPAM shell undergoes collapsing at elevated temperatures (Figure 1a). Thus, increasing temperature will lead to the formation of more densely packed nanoparticles within the unimolecular micelles. UV−vis absorption proved to be a convenient technique to monitor the shift of surface plasmon resonance (SPR) band and the change in the spatial distribution of nanoparticles. Tenhu et al.[17b] studied the optical properties of PNIPAM-coated gold nanoparticles. When the nanoparticles formed a monolayer on the air−water surface, the SPR band exhibited a blue-shift during the monolayer compression due to the conformational changes of coated PNIPAM chains. Multilayers were formed through successive deposition of monolayers of gold nanoparticles. These workers also found that multilayers deposited at higher temperatures (thinner PNIPAM coating layers) exhibited more prominent red-shifts compared to those deposited at lower temperatures.

Temperature-dependent UV−vis spectra of hybrid unimolecular micelles prepared at low and high dosages of $AgNO_3$ are shown in Figure 6. It reveals that increasing temperature leads to a clear red-shift of the surface plasmon band of silver composite nanoparticles. The reasons for this red-shift might be twofold, which is similar to that observed in the PNIPAM-based hybrid microgel systems.[10a,20] First, as temperature increases, the shrinkage of the PNIPAM shell in the unimolecular micelles decreases the relative distances between neighboring Ag nanoparticles, leading to stronger interparticle coupling.[17b] Second, the refractive index of the PNIPAM chain segments surrounding Ag nanoparticles increases with temperature, owing to the expelling of water molecules from the polymer shell upon shrinkage.

We can also tell from Figure 6 that hybrid unimolecular micelles with higher number density of Ag nanoparticles (Figure 6b) exhibits a more dramatic red-shift of surface plasmon peak (from 398 to 412 nm) as compared to that prepared at low

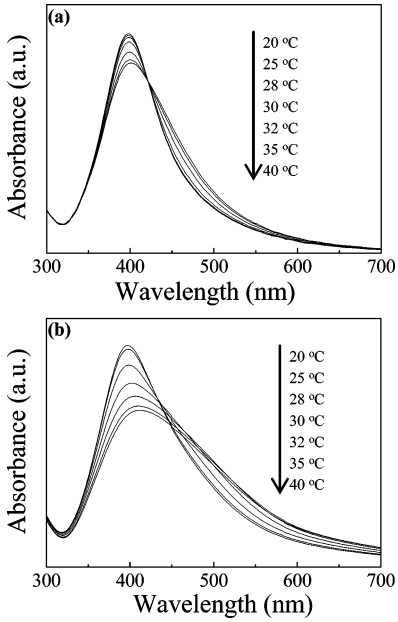

Figure 6. UV−vis spectra of hybrid unimolecular micelles with different silver dosages (a: low dosage; b: high dosage) measured at different temperatures. The unimolecular micelles concentration was 1×10^{-5} g/mL.

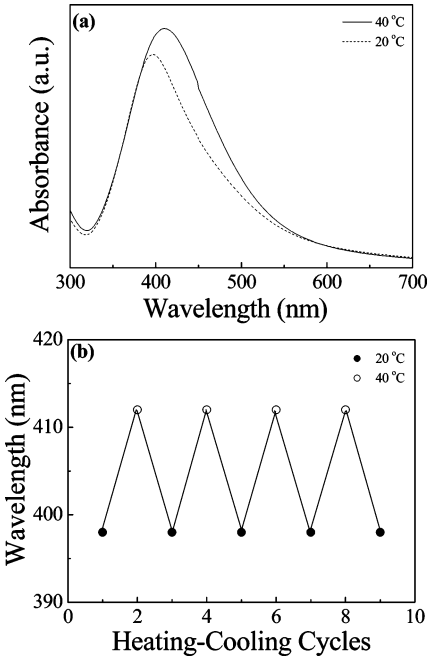

Figure 7. (a) UV−vis absorption spectra of hybrid unimolecular micelles (prepared at high dosage of $AgNO_3$) as the temperature decreases from 40 °C (solid line) to 20 °C (dashed line). (b) Maximum wavelength of the surface plasmon peak as a function of the heating−cooling cycles between 20 and 40 °C. The H40-PNIPAM concentration was 1×10^{-5} g/mL.

dosage (Figure 6a, from 398 to 402 nm). Previous results indicate that the change of refractive index can induce the red-shift of surface plasmon peak only up to 5 nm even though the external temperature is increased to 60 °C.[20] So the dramatic red-shift at increasing temperatures for hybrid unimolecular micelles prepared at high dosage (Figure 6b) is mainly due to the decrease of relative distances between silver nanoparticles and enhanced interparticle coupling, which is driven by the shrinkage of PNIPAM brush of unimolecular micelles (Figure 1a).

The temperature-induced red-shift of the surface plasmon peak is completely reversible (see Figure 7). Upon cooling from 40 to 20 °C, the plasmon peak shifts back to their original position at 20 °C, and it red-shifts to ∼412 nm again when the temperature increases back to 40 °C. The complete reversibility also proves that there is no coagulation between Ag nanoparticles during the heating/cooling cycles. Thus, the spatial distances between adjacent Ag nanoparticles could be reversibly tuned with temperature.

In summary, we have successfully established that embedding silver nanoparticles into thermoresponsive unimolecular micelles can lead to the convenient and reversible thermotuning of the spatial distribution of nanoparticles. In this way, the immobilized nanoparticles can act as an "indicator" of external conditions. If the prepared silver composite nanoparticles are to be used as a "nanoreactor" for catalytic applications, the permeability of the PNIPAM shell to reactants can be adjusted to be open or close at low and high temperatures, respectively. It can be envisioned that the hybrid unimolecular micelles could act as a chemical or biochemical monitor/indicator of a specific chemical or biochemical species on the basis of the surface plasmon peak shifts. We also surmise that this novel hybrid system could find applications in the highly sensitive and selective sensors, high-performance catalysis, and smart optic/electronic devices.

Acknowledgment. This work was supported by an Outstanding Youth Fund (50425310) and a key research grant (20534020) from the National Natural Scientific Foundation of China (NNSFC), the "Bai Ren" Project of the Chinese Academy of Sciences, and the Program for Changjiang Scholars and Innovative Research Team in University (PCSIRT).

References and Notes

(1) (a) Maier, S. A.; Brongersma, M. L.; Kik, P. G.; Meltzer, S.; Requicha, A. A. G.; Atwater, H. A. *Adv. Mater.* **2001**, *13*, 1501. (b) Chen, S.; Yang, Y. *J. Am. Chem. Soc.* **2002**, *124*, 5280. (c) Trindade, T.; O'Brien, P.; Pickett, N. L. *Chem. Mater.* **2001**, *13*, 3843.

(2) (a) Taton, T. A.; Mirkin, C. A.; Letsinger, R. L. *Science* **2000**, *289*, 1757. (b) Peng, X. G.; Xiao, M. *Nano Lett.* **2003**, *3*, 819. (c) Shipway, A. N.; Katz, E.; Willner, J. *ChemPhysChem* **2000**, *1*, 18.

(3) (a) Campell, C. T.; Parker, S. C.; Starr, D. E. *Science* **2002**, *298*, 811. (b) Zhao, M.; Crooks, R. M. *Angew. Chem., Int. Ed.* **1999**, *38*, 364. (c) Lewis, L. N. *Chem. Rev.* **1993**, *93*, 2693.

(4) (a) Daniel, M. C.; Astruc, D. *Chem. Rev.* **2004**, *104*, 293. (b) Schultz, D. *Curr. Opin. Biotechnol.* **2003**, *14*, 13. (c) You, C. C.; Verma, A. V.; Rotello, M. *Soft Matter* **2006**, *2*, 190.

(5) (a) Tang, Z.; Kotov, N. A. *Adv. Mater.* **2005**, *17*, 951. (b) Hammond, P. T. *Adv. Mater.* **2004**, *16*, 1271. (c) Lopes, W. A.; Jaeger, H. M. *Nature (London)* **2001**, *414*, 735.

(6) (a) Filali, M.; Meier, M. A. R.; Schuber, U. S.; Gohy, J. F. *Langmuir* **2005,** *21*, 7995. (b) Kang, Y.; Taton, T. A. *Angew. Chem., Int. Ed.* **2005**, *44*, 409. (c) Zhao, H.; Douglas, E. P. *Chem. Mater.* **2002**, *14*, 1418. (d) Liu, S. Y.; Weaver, J. V. M.; Save, M.; Armes, S. P. *Langmuir* **2002**, *18*, 8350.

(7) (a) Crooks, R. M.; Zhao, M.; Sun, L.; Chechik, V.; Yeung, L. K. *Acc. Chem. Res.* **2001**, *34*, 181. (b) Scott, R. W. J.; Wilson, O. M.; Crooks, R. M. *J. Phys. Chem. B* **2005**, *109*, 692. (c) Shifrina, Z. B.; Rajadurai, M. S.; Firsova, N. V.; Bronstein, L. M.; Huang, X.; Rusanov, A. L.; Muellen, K. *Macromolecules* **2005**, *38*, 9920. (d) Worden, J. G.; Dai, Q.; Huo, Q. *Chem. Commun.* **2006**, 1536.

(8) (a) Chen, C. W.; Chen, M. Q.; Serizawa, T.; Akashi, M. *Adv. Mater.* **1998**, *10*, 1122. (b) Lu, Y.; Mei, Y.; Drechsler, M.; Ballauff, M. *Angew. Chem., Int. Ed.* **2006**, *45*, 813. (c) Cen, L.; Neoh, K. G.; Kang, E. T. *Adv. Mater.* **2005**, *17*, 1656.

(9) (a) Zhang, J. G.; Xu, S. Q.; Kumacheva, E. *J. Am. Chem. Soc.* **2004**, *126*, 7908. (b) Zhang, J. G.; Xu, S. Q.; Kumacheva, E. *Adv. Mater.* **2005**, *17*, 2336. (c) Pich, A.; Karak, A.; Lu, Y.; Ghosh, A. K.; Adler, H.-J. *Macromol. Rapid Commun.* **2006**, *27*, 344. (d) Pich, A.; Hain, J.; Lu, Y.; Boyko, V.; Prots, Y.; Adler, H.-J. *Macromolecules* **2005**, *38*, 6610.

(10) (a) Li, J.; Hong, X.; Liu, Y.; Wang, Y. W.; Li, J. H.; Bai, Y. B.; Li, T. J. *Adv. Mater.* **2005**, *17*, 163. (b) Kuang, M.; Wang, D. Y.; Bao, H. B.; Gao, M. Y.; Mohwald, H.; Jiang, M. *Adv. Mater.* **2005**, *17*, 267. (c) Suzuki, D.; Kawaguchi, H. *Langmuir* **2006**, *22*, 3818. (d) Pich, A.; Bhattacharya, S.; Lu, Y.; Boyko, V.; Adler, H.-J. *Langmuir* **2004**, *20*, 10706.

(11) (a) Sakai, T.; Alexanderidis, P. *Langmuir* **2005**, *21*, 8019. (b) Bronstein, L. M.; Sidorov, S. N.; Zhirov, V.; Zhirov, D.; Kabachii, Y. A.; Kochev, S. Y.; Valetsky, P. M.; Stein, B.; Kiseleva, O. I.; Polyakov, S. N.; Shtykova, E. V.; Nikulina, E. V.; Svergun, D. I.; Khokhlov, A. R. *J. Phys. Chem. B* **2005**, *109*, 18786. (c) Lefebvre, M. D.; Shull, K. R. *Macromolecules* **2006**, *39*, 3450.

(12) (a) Hawker, C. J.; Wooley, K. L.; Frechet, J. M. J. *J. Chem. Soc., Perkin Trans. 1* **1993**, 1287. (b) You, Y. Z.; Hong, C. Y.; Pan, C. Y.; Wang, P. H. *Adv. Mater.* **2004**, *16*, 1953. (c) Heise, A.; Hedrick, J. L.; Frank, C. W.; Miller, R. D. *J. Am. Chem. Soc.* **1999**, *121*, 8647. (d) Haag, R. *Angew. Chem., Int. Ed.* **2004**, *43*, 278. (e) Gillies, E. R.; Frechet, J. M. J. *Drug Discov. Today* **2005**, *10*, 35. (f) Liu, M.; Kono, K.; Frechet, J. M. J. *J. Controlled Release* **2000**, *65*, 121. (g) Aathimanikandan, S. V.; Savariar, E. N.; Thayumanavan, S. *J. Am. Chem. Soc.* **2005**, *127*, 14922.

(13) Schild, H. G. *Prog. Polym. Sci.* **1992**, *17*, 163.

(14) (a) Xu, J.; Luo, S. Z.; Shi, W. F.; Liu, S. Y. *Langmuir* **2006**, *22*, 989. (b) Luo, S. Z.; Xu, J.; Zhu, Z. Y.; Wu, C.; Liu, S. Y. *J. Phys. Chem. B* **2006**, *110*, 9132.

(15) (a) Ornatska, M.; Peleshanko, S.; Rybak, B.; Holzmueller, J.; Tsukruk, V. V. *Adv. Mater.* **2004**, *16*, 2206. (b) Ornatska, M.; Peleshanko, S.; Genson, K. L.; Rybak, B.; Bergman, K. N.; Tsukruk, V. V. *J. Am. Chem. Soc.* **2004**, *126*, 9675. (c) Ornatska, M.; Bergman, K. N.; Rybak, B.; Peleshanko, S.; Tsukruk, V. V. *Angew. Chem., Int. Ed.* **2004**, *126*, 5246.

(16) Sehgal, R. K.; Kumar, S. *Org. Prep. Proc. Int.* **1989**, *21*, 223.

(17) (a) Shan, J.; Chen, J.; Nuopponen, M.; Tenhu, H. *Langmuir* **2004**, *20*, 4671. (b) Shan, J.; Chen, J.; Nuopponen, M.; Viitala, T.; Jiang, H.; Peltonen, J.; Kauppinen, E.; Tenhu, H. *Langmuir* **2006**, *22*, 794.

(18) Kamat, P. V. *J. Phys. Chem. B* **2002**, *106*, 7729.

(19) Lu, Y.; Mei, Y.; Ballauff, M.; Drechesler, M. *J. Phys. Chem. B* **2006**, *110*, 3930.

(20) Kuang, M.; Wang, D. Y.; Mohwald, H. *Adv. Funct. Mater.* **2005**, *15*, 1611.

MA061584D